



Cite this: *Chem. Sci.*, 2021, **12**, 12326

All publication charges for this article have been paid for by the Royal Society of Chemistry

Received 27th May 2021
Accepted 13th August 2021

DOI: 10.1039/d1sc02873a
rsc.li/chemical-science

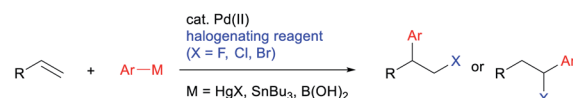
Introduction

Development of new methodologies for the highly efficient, selective preparation of complex compounds is an important issue in current organic synthesis.¹ Catalytic difunctionalization of alkenes has progressed to open new avenues for the introduction of diverse functionalities into easily accessible chemical feedstock.² Given that halogenated organic compounds are valuable materials and have desirable properties,³ the transition-metal-catalyzed carbohalogenation of alkenes represents a potent approach for preparing multiply substituted alkyl halides.⁴ A traditional and reliable method for this type of catalytic carbohalogenation is the use of aryl metal reagents in combination with halogenating reagents (Scheme 1a). In 1968, Heck reported on the Pd-catalyzed 1,2-arylhalogenation of alkenes using aryl mercury reagents in the presence of copper halides.⁵ Yoshida subsequently reported on a preliminary example of the Pd-catalyzed 1,1-arylchlorination of terminal alkenes using aryl tributylstannanes and CuCl₂.⁶ Following these prior reports, Sanford developed a general protocol for the Pd-catalyzed 1,1- and 1,2-arylhalogenation of terminal alkenes with aryl tributylstannanes, in which the regioselectivities can be controlled by fine-tuning the halogenation reagents, the reaction conditions, and the alkene substituents.⁷ The use of aryl boronic acids with electrophilic fluorination reagents has also been reported for the Pd-catalyzed 1,1-arylfluorination of alkenes,⁸ and this method is applicable to 1,2-arylfluorination in combination with directing groups.⁹ Mechanistic studies on the reported 1,1-arylhalogenations suggest that a β -hydride elimination/reinsertion process

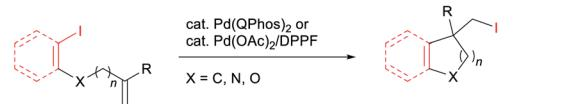
was involved and that the resulting π -benzyl Pd intermediate facilitated a 1,1-selective reaction.^{7b,8}

In contrast, carbohalogenation reactions that involve the direct addition of a carbon–halogen bond to an alkene is a more atom-economical approach to providing alkyl halides. In 2011, Lautens^{10a} and Tong^{10b} independently reported on the Pd(0)-catalyzed intramolecular 1,2-addition of C(sp²)–I bonds to alkenes using QPhos or DPPF as ligands (Scheme 1b). Their reports triggered the development of the catalytic intramolecular 1,2-addition of C(sp²)–I bonds to alkenes utilizing not only Pd¹⁰ but also Ni¹¹ catalysts. A key to the success of these

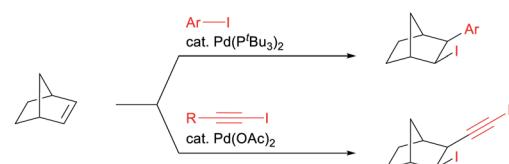
a) 1,1- and 1,2-arylation of alkenes with aryl metal reagents in the presence of halogenating reagents (refs 5–9)



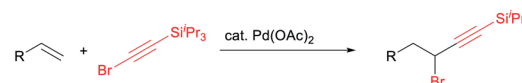
b) intramolecular 1,2-carboiodination of alkenes with aryl or alkynyl iodides (refs 10a, 10b)



c) 1,2-carboiodination of norbornene with aryl or alkynyl iodides (refs 10a, 12)



d) the first 1,1-alkynylbromination of alkenes with alkynyl bromides (this work)



^aDepartment of Applied Chemistry, Faculty of Engineering, Osaka University, 2-1 Yamadaoka, Suita, Osaka 565-0871, Japan. E-mail: ano@chem.eng.osaka-u.ac.jp

^bCenter for Atomic and Molecular Technologies, Graduate School of Engineering, Osaka University, 2-1 Yamadaoka, Suita, Osaka 565-0871, Japan

† Electronic supplementary information (ESI) available. See DOI: [10.1039/d1sc02873a](https://doi.org/10.1039/d1sc02873a)

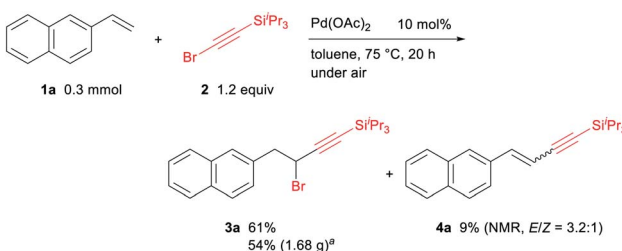
Scheme 1 Palladium-catalyzed carbohalogenation of alkenes.



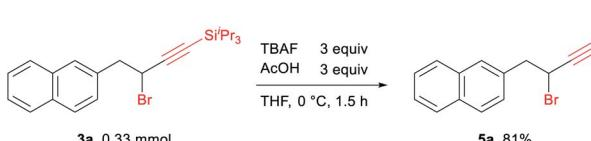
reactions is the introduction of a substituent on the internal carbon atom of the alkene, which inhibits the undesirable β -hydride elimination process by forming a quaternary carbon center. Norbornene can be employed for Pd-catalyzed intermolecular 1,2-carboiodination reactions using aryl iodides^{10a} or alkynyl iodides¹² (Scheme 1c). The Pd¹³- and Ni¹⁴-catalyzed carbohalogenation of internal alkynes has also recently been developed using aryl halides. To the best of our knowledge, however, the catalytic 1,1-addition of organohalides to alkenes has not been reported so far. Moreover, except for the C–I bond, the addition of a C–halogen bond to alkenes continues to be a challenging issue in the Pd-catalyzed reaction.^{10f,15,16} Herein, we report on the first example of the Pd-catalyzed 1,1-alkynylbromination of terminal alkenes with alkynyl bromides (Scheme 1d).

Results and discussion

We initially investigated the Pd-catalyzed alkynylbromination of 2-vinylnaphthalene (**1a**) with alkynyl bromide **2** as a model reaction. To our delight, the 1,1-alkynylbromination product **3a** was obtained in 71% NMR yield and 61% isolated yield when **1a** (0.3 mmol) was reacted with **2** (1.2 equiv.) in the presence of Pd(OAc)₂ (10 mol%) in toluene (1 mL) at 75 °C for 20 h under air (Scheme 2). It should be noted that the 1,2-alkynylbromination product of **1a** was not observed, while a Mizoroki–Heck type reaction of **1a** with **2** took place to give the alkynylalkene **4a** in 9% NMR yield as a *E/Z* mixture (*E/Z* = 3.2 : 1). Extensive optimization studies revealed that neither the addition of ligands, bases, and acids nor the use of other solvents was effective for improving the yield of **3a**.¹⁷ In a gram-scale reaction using 1.16 g (7.5 mmol) of **1a** under the optimal reaction conditions, 1.68 g of **3a** was produced in 54% yield. Removal of the triisopropylsilyl group from **3a** was also successful using TBAF/AcOH in THF at 0 °C, giving the corresponding terminal alkyne **5a** in 81% yield (Scheme 3).

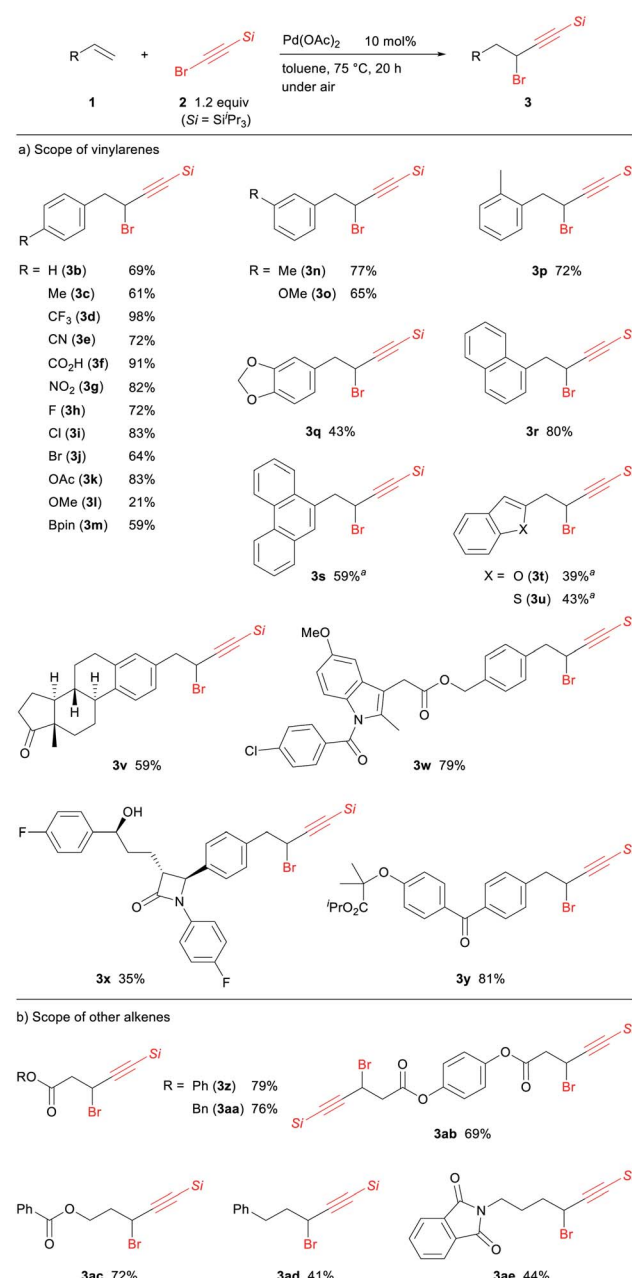


Scheme 2 Optimal reaction conditions for the Pd-catalyzed 1,1-alkynylbromination of **1a** with **2**. ^a1.16 g (7.5 mmol) of **1a** was used.



Scheme 3 Removal of triisopropylsilyl group.

Having established the optimal reaction conditions, we explored the scope of vinylarenes toward the Pd-catalyzed 1,1-alkynylbromination (Scheme 4a). This reaction tolerates a wide variety of functional groups and substitution patterns on the aromatic ring. For example, both electron-withdrawing (**1d–g**) and electron-donating (**1c**, **1k**, **1n**, **1o**) groups were compatible for this catalytic 1,1-alkynylbromination, giving the corresponding propargylic bromides in good yields. The reaction of styrenes bearing halogen (**1h–j**) or boronate (**1m**) groups was also successful with these functionalities remaining intact, which would be useful for further functionalization by cross-



Scheme 4 Scope of the reaction. Reaction conditions: alkene (**1**, 0.3 mmol), alkynyl bromide (**2**, 0.36 mmol), Pd(OAc)₂ (0.03 mmol), toluene (1 mL), 75 °C, 20 h, under air. ^aRun for 48 h.



coupling protocols. In contrast, the reaction of the electron-rich **1l** and **1q** was impeded by competitive oligomerization under the optimal conditions, leading to decreased yields. Sterically demanding vinylarenes such as **1p** and **1r** were applicable to this reaction, while a longer time was required for the 1,1-alkynylbromination of 9-vinylphenanthrene (**1s**) to reach completion. The 1,1-alkynylbromination of vinylheteroarenes **1t** and **1u** proceeded slowly along with their partial decomposition, resulting in only moderate yields. It should be noted that this protocol could also be applied to vinylarenes derived from biologically active compounds or pharmaceuticals. For example, the estrone (**3v**), indomethacin (**3w**), ezetimibe (**3x**), and fenofibrate (**3y**) that contained a propargylic bromide core could be easily synthesized.

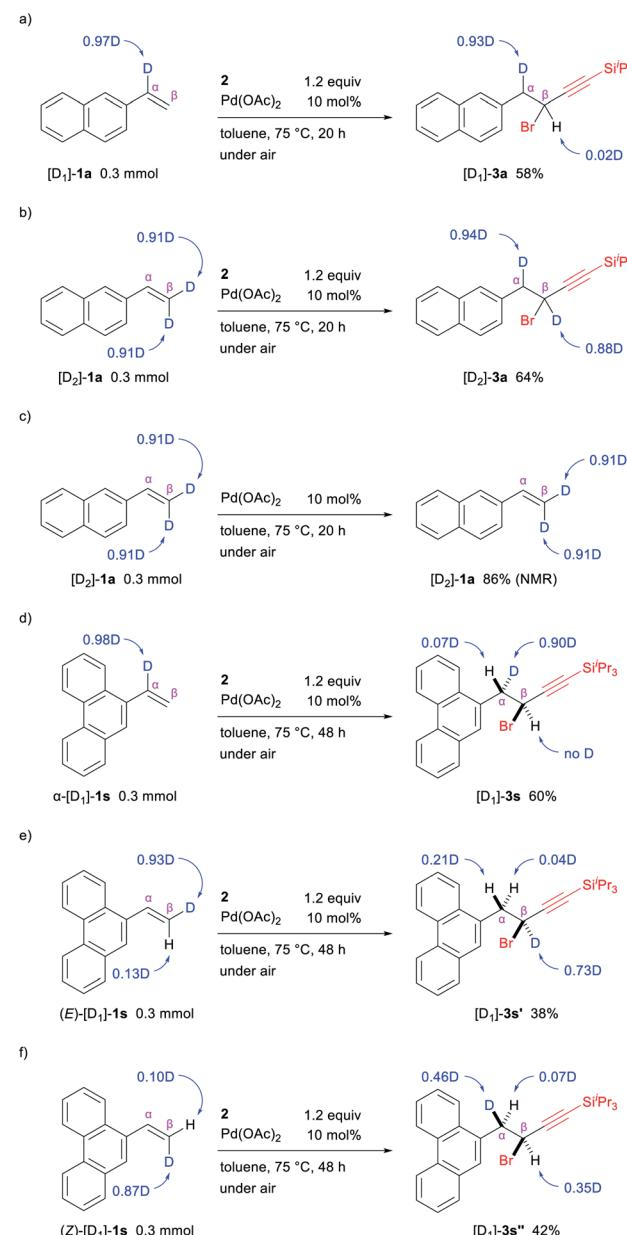
We next evaluated the reactivity of other alkenes under the optimal conditions (Scheme 4b). Acrylates such as **1z** and **1aa** could be employed for this 1,1-alkynylbromination protocol, and bis-1,1-alkynylbromination of **1ab** was also successful, giving **3ab** as the sole product in good yield. To our surprise, the reaction of allyl benzoate **1ac** afforded **3ac** without the elimination of the benzoate moiety.¹⁸ Electronically unbiased alkenes such as **1ad** and **1ae** could be used in the 1,1-alkynylbromination, but the yields of **3ad** and **3ae** remained moderate due to the competitive alkene isomerization. Unfortunately, internal alkenes were unreactive under the optimal conditions.

Monitoring the progress of the 1,1-alkynylbromination of **1a** by ¹H NMR revealed that there was an induction period at the initial stage of the reaction under the optimal conditions, whereas no induction period was involved when the reaction was conducted with $\text{Pd}_2(\text{dba})_3 \cdot \text{CHCl}_3$ instead of $\text{Pd}(\text{OAc})_2$ (see the ESI†). This result indicated that a $\text{Pd}(0)$ species, generated through the stoichiometric Wacker-type oxidation of **1a** with $\text{Pd}(\text{OAc})_2$,^{19,20} was likely an active species.

A plausible reaction pathway is illustrated in Scheme 5. To the $\text{Pd}(0)$ species generated by reduction of $\text{Pd}(\text{OAc})_2$, the oxidative addition of the alkynyl bromide **2** takes place to afford the alkynylpalladium bromide **A**. Coordination of alkene **1** to **A**

forms **B**, and the migratory insertion of **1** into the $\text{Pd}-\text{C}(\text{sp})$ bond of **B** gives intermediate **C**. A subsequent β -hydride elimination followed by reinsertion of the alkynylalkene into $\text{Pd}-\text{H}$ bond leads to the migration of a $\text{Pd}(\text{II})$ center to form intermediate **E**. Finally, reductive elimination to form a $\text{C}(\text{sp}^3)-\text{Br}$ bond gives the 1,1-alkynylbromination product **3** along with the generation of $\text{Pd}(0)$.

To gain further insights into the mechanism for this reaction, the 1,1-alkynylbromination of deuterated 2-vinyl-naphthalenes was examined under the optimal conditions. The reaction of $[\text{D}_1]-\text{1a}$ (0.97D at the α -carbon) with **2** gave $[\text{D}_1]-\text{3a}$ in 58% yield with the deuterium incorporation at the α -carbon being retained (Scheme 6a). On the other hand, when $[\text{D}_2]-\text{1a}$ bearing two deuterium atoms at the β -carbon (both are 0.91D



Scheme 5 A plausible mechanism ($\text{Si} = \text{Si}^{\text{i}}\text{Pr}_3$).

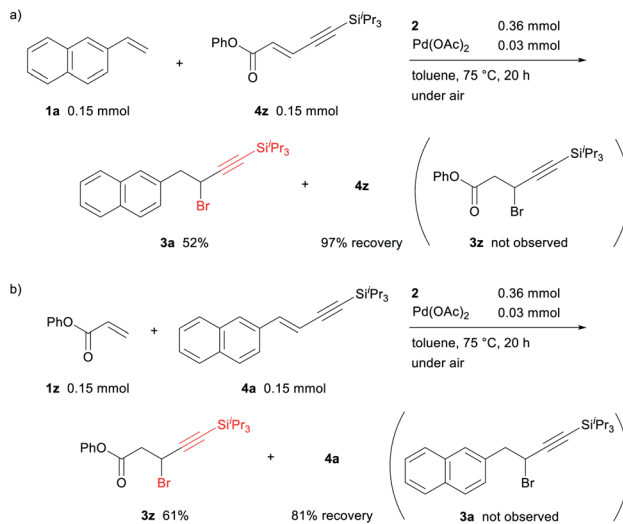
Scheme 6 Deuterium-labelling experiments.



incorporation) was used, the reaction proceeded without the loss of deuterium atoms and afforded $[D_2]$ -**3a** in which one deuterium atom remained at the β -carbon (0.88D) and the other was observed to be located on the α -carbon (0.94D) (Scheme 6b). In addition, no loss of deuterium atoms was observed when the reaction of $[D_2]$ -**1a** was carried out in the absence of **2** (Scheme 6c). These results indicate that a deuterium atom at the β -carbon of the alkene migrated to the α -carbon during the reaction, which was consistent with a mechanism involving β -hydride elimination followed by reinsertion (**C** \rightarrow **D** \rightarrow **E**, in Scheme 5).²¹

Interest in the stereochemical course of the reaction prompted us to perform some deuterium-labelling experiments using **1s**, in which the 1,1-alkynylbromination product **3s** has diastereotopic benzylic protons that can be distinguished by ^1H NMR analysis. Similar to the reaction of $[D_1]$ -**1a**, the reaction of α - $[D_1]$ -**1s** (0.98D at the α -carbon) with **2** proceeded while the deuterium incorporation at the α -carbon being retained, giving $[D_1]$ -**3s** in 60% yield (Scheme 6d). The configuration between this deuterium atom and the hydrogen atom at the β -carbon in $[D_1]$ -**3s** was assigned as *syn* based on ^1H NMR analysis. Furthermore, the reaction of (*E*)- $[D_1]$ -**1s** (0.93D and 0.13D at the *E*- and *Z*-position, respectively) afforded $[D_1]$ -**3s'** in which the deuterium was mainly at the β -carbon (0.73D), while a partial incorporation of deuterium at the α -carbon (0.21D) also occurred in an *anti*-configuration with respect to the deuterium atom at the β -carbon (Scheme 6e). This result suggests that the major reaction pathway involves the cleavage of the C–H bond at the *Z*-position to the 9-phenanthrenyl group by β -hydride elimination. In the light of the *syn*-stereochemical course for the migratory insertion of alkenes to Pd–C(sp) bond²² and β -hydride elimination/reinsertion,²³ the findings for these deuterium-labelling experiments suggest that the reductive elimination of the C(sp³)–Br bond likely proceeds with retention of configuration, as shown in Scheme 7. We also examined the 1,1-alkynylbromination of (*Z*)- $[D_1]$ -**1s** (0.10D and 0.87D at *E*- and *Z*-position, respectively) with the expectation that the reaction would proceed *via* the migration of the deuterium atom from the β -carbon to the α -carbon. However, this reaction provided $[D_1]$ -**3s''** with deuterium scrambling (Scheme 6f), indicating that another reaction pathway appears to be involved as a minor pathway in this 1,1-alkynylbromination.²⁴

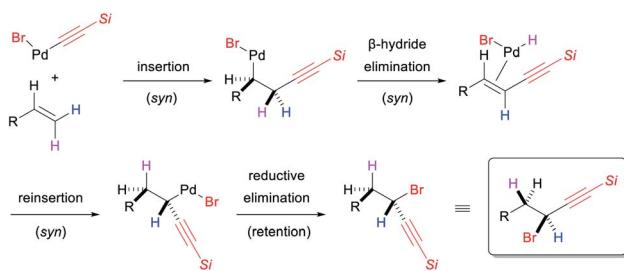
A crossover experiment using an equimolar mixture of **1a** and the alkynylalkene **4z**, provided by Mizoroki–Heck type reaction of **1z** with **2**, afforded **3a** in 52% yield along with 97% of



Scheme 8 Crossover experiments.

4z being recovered (Scheme 8a). Similarly, using an equimolar mixture of **1z** and alkynylalkene **4a** in the reaction resulted in the formation of **3z** as the sole 1,1-alkynylbromination product with 81% of **4a** being recovered (Scheme 8b). These results indicate that the coordinating alkynylalkene **4** in intermediate **D** is reinserted into the Pd–H bond without exchanging a free alkynylalkene (Scheme 5).

In an attempt to shed light on the unusual regioselectivity of this reaction, we calculated the Gibbs free energy profiles for the 1,1-alkynylbromination of **1b** with the alkynyl bromide **2'** at the SMD (toluene) M06L/def2TZVP//B3LYP/6-31G(d)–LANL2DZ (for Pd and Br) level of theory.^{25,26} The calculated Gibbs free energy profiles are shown in Fig. 1a, where a Pd(0)/**2'** complex **INT0** was set as the relative zero point. The initial oxidative addition of **2'** on the Pd(0) center of **INT1** proceeds *via* **TS₁₋₂** with an energy barrier of 24.9 kcal mol^{–1}, providing the three-coordinated intermediate **INT2**. In **TS₁₋₂**, the lengths of the cleaving C–Br bond and the forming Pd–Br bond are 2.23 and 2.70 Å, respectively (Fig. 1b). The coordination of **1b** to **INT2** gives **INT3** along with an energy release of 8.7 kcal mol^{–1}, and the following migratory insertion of **1b** into the Pd–C bond *via* **TS₃₋₄** requires an activation barrier of 12.9 kcal mol^{–1}, giving the benzyl Pd intermediate **INT4**. The computed structure of **TS₃₋₄** shows that the lengths of the forming C–C bond and the breaking Pd–C bond are 2.06 and 2.00 Å, respectively. The subsequent C–C bond rotation in **INT4** gives **INT5** along with the dissociation of the alkyne moiety from the Pd center. The migration of Pd from the benzylic position (**INT5**) to the propargylic position (**INT8**) is initiated by a β -hydride elimination *via* **TS₅₋₆** with an activation barrier of 14.3 kcal mol^{–1} to give **INT6**. The computational results showed that **TS₇₋₈** for the migratory reinsertion of the coordinating alkynylalkene into the Pd–H bond requires higher activation energy than that for **TS₅₋₆** ($\Delta\Delta G^\ddagger = 2.3$ kcal mol^{–1}) and the overall energy barrier for the Pd migration step is 16.6 kcal mol^{–1}. The σ -propargyl Pd intermediate **INT8** can be converted into the π -allenyl Pd intermediate **INT9** with an exothermal energy of 6.9 kcal mol^{–1}. It should be noted that the



Scheme 7 A plausible stereochemistry of the reaction (*Si* = *Si*Pr₃).



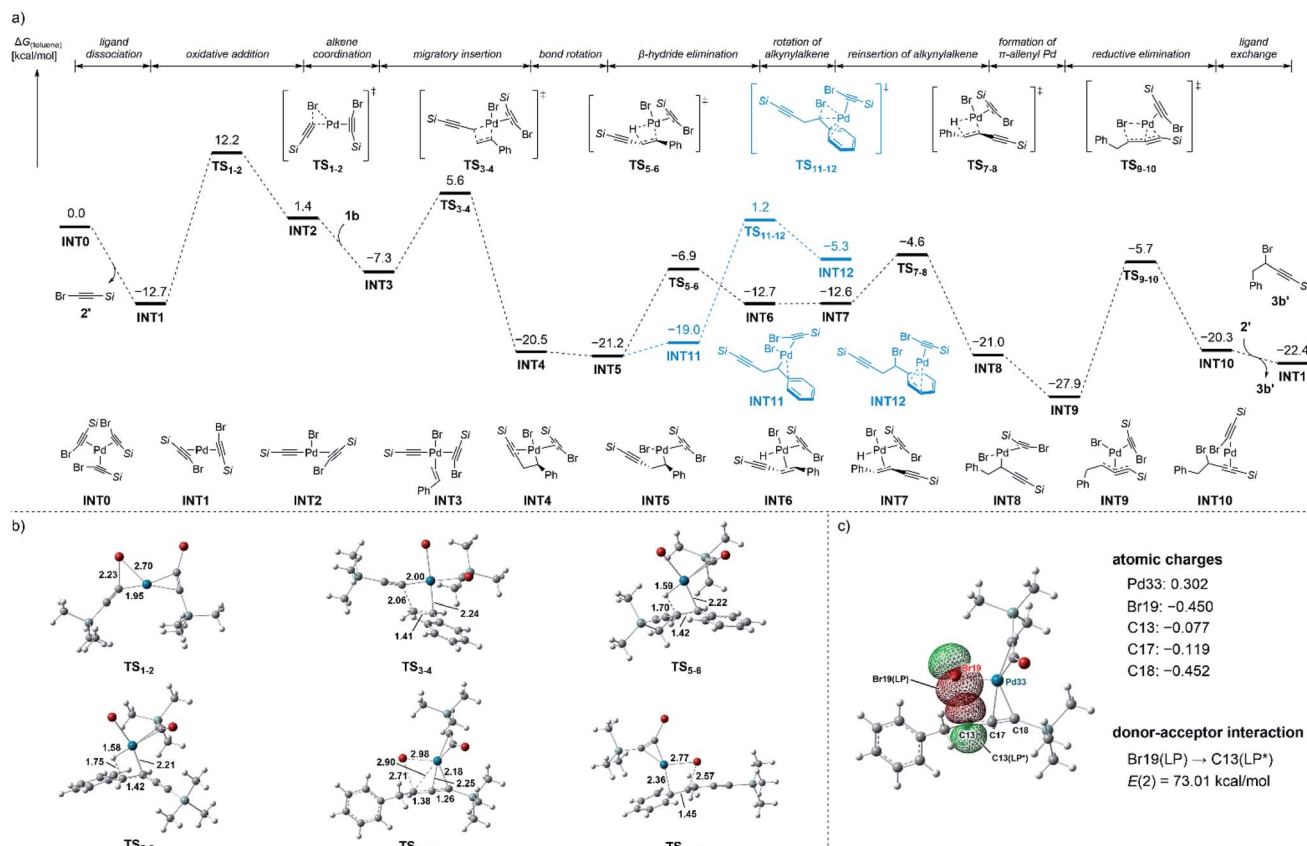


Fig. 1 (a) Gibbs free energy profiles for the Pd-catalyzed 1,1-alkynylbromination of **1b** with **2'** (*Si* = *SiMe*₃). (b) Optimized structures of TSs. (c) Natural population analysis of **TS**₉₋₁₀.

π-allenyl Pd intermediate **INT9** was found to be 6.7 kcal mol⁻¹ more thermodynamically stable than the σ-benzyl Pd intermediate **INT5**.

The reductive elimination proceeds from **INT9** via **TS**₉₋₁₀ with an activation barrier of 22.2 kcal mol⁻¹, and **INT10** is formed with retention of configuration at the propargylic carbon atom,²⁷ which is consistent with the observations from our deuterium-labelling experiments (Scheme 6). Structural information regarding **TS**₉₋₁₀ shows that the length of the cleaving Pd–Br bond is 2.98 Å and that of the forming C–Br bond is 2.71 Å, and the propargylic carbon is a distance of 2.90 Å from the Pd center. The geometry of **TS**₉₋₁₀ suggests that the reductive elimination likely proceeds via the release of the bromine ligand from Pd center prior to the formation of the C–Br bond. This mechanism is in agreement with the reverse process of the oxidative addition of propargylic halides to zero-valent group 10 metal complexes.²⁸ Fig. 1c shows the result of the natural population analysis (NPA) of **TS**₉₋₁₀, where the values of the natural charges for Pd33 and Br19 atoms were found to be 0.302 and -0.450, respectively, while the negative charge on the allenyl moiety was distributed on C18 (C13, -0.077; C17, -0.119; C18, -0.452). Moreover, the natural bond orbital (NBO) analysis²⁹ of **TS**₉₋₁₀ revealed that the donor–acceptor interaction from the p-orbital of the Br19 atom to the p-orbital of the C13 atom was large, which also supports the above mechanism. Finally, ligand

exchange provides **3b'** and **INT1** along with an exothermal energy of 2.1 kcal mol⁻¹. The calculations also revealed that the reductive elimination of C(benzyl)–Br bond from **INT11** occurs via **TS**₁₁₋₁₂, the free energy of which is higher than that of **TS**₇₋₈ and **TS**₉₋₁₀ ($\Delta\Delta G^\ddagger$ = 5.8 and 6.9 kcal mol⁻¹, respectively), indicating that the formation of 1,2-alkynylbromination product is a kinetically unfavourable process.

Conclusions

In summary, we report on the first Pd-catalyzed 1,1-alkynylbromination of terminal alkenes using a silyl-protected alkynyl bromide as an alkynylbromination reagent. A variety of alkenes including vinylarenes, acrylates, and electronically unbiased alkenes were found to be applicable to this protocol thus providing direct access to functionalized propargylic bromides. Deuterium-labelling experiments revealed that the migration of a Pd center is involved in the formation of the 1,1-alkynylbromination product and suggest that the reductive elimination proceeds with the retention of configuration. Computational studies also support that the conclusion that the reductive elimination occurs from a π-allenyl Pd intermediate and that the C–Br bond is formed in a stereoretentive fashion at the propargylic carbon atom. Further mechanistic studies are currently underway in our group.

Data availability

All experimental data and detailed procedures are available in the ESI.†

Author contributions

Y. A. conceived the study, carried out the computations, and wrote the manuscript. N. K. performed the experiments and analyzed the data. N. C. discussed the results with Y. A. and N. K. All authors commented on the manuscript.

Conflicts of interest

There are no conflicts to declare.

Acknowledgements

This work was supported by Grant-in-Aid for Early-Career Scientists (18K14218 to Y. A.) and Grant-in-Aid for Specially Promoted Research (17H06091 to N. C.) from JSPS. We thank the Analytical Instrumentation Facility, Graduate School of Engineering, Osaka University, for their assistance with HRMS.

Notes and references

- (a) B. M. Trost, *Science*, 1983, **219**, 245–250; (b) P. A. Wender and B. L. Miller, *Nature*, 2009, **460**, 197–201; (c) Q.-L. Zhou, *Angew. Chem., Int. Ed.*, 2016, **55**, 5352–5353; (d) J. R. Ludwig and C. S. Schindler, *Chem.*, 2017, **2**, 313–316.
- For recent reviews on catalytic difunctionalization of alkenes, see: (a) J.-S. Zhang, L. Liu, T. Chen and L.-B. Han, *Chem. – Asian J.*, 2018, **13**, 2277–2291; (b) Y. Li, D. Wu, H.-G. Cheng and G. Yin, *Angew. Chem., Int. Ed.*, 2020, **59**, 7990–8003; (c) J. Derosa, O. Apolinar, T. Kang, V. T. Tran and K. M. Engle, *Chem. Sci.*, 2020, **11**, 4287–4296; (d) R. K. Dhungana, R. R. Sapkota, D. Niroula and R. Giri, *Chem. Sci.*, 2020, **11**, 9757–9774.
- For selected reviews on halogenated bioactive compounds and natural products, see: (a) C. Wagner, M. El Omari and G. M. König, *J. Nat. Prod.*, 2009, **72**, 540–553; (b) P. M. Pauletti, L. S. Cintra, C. G. Braguine, A. A. da Silva Filho, M. L. A. e. Silva, W. R. Cunha and A. H. Januário, *Mar. Drugs*, 2010, **8**, 1526–1549; (c) G. W. Gribble, *Environ. Chem.*, 2015, **12**, 396–405; (d) G. W. Gribble, *Mar. Drugs*, 2015, **13**, 4044–4136; (e) W.-J. Chung and C. D. Vanderwal, *Angew. Chem., Int. Ed.*, 2016, **55**, 4396–4434.
- For recent reviews on the formation of carbon–halogen bonds, see: (a) X. Jiang, H. Liu and Z. Gu, *Asian J. Org. Chem.*, 2012, **1**, 16–24; (b) C. Chen and X. Tong, *Org. Chem. Front.*, 2014, **1**, 439–446; (c) M. G. Campbell and T. Ritter, *Chem. Rev.*, 2015, **115**, 612–633; (d) D. A. Petrone, C. M. Le, S. G. Newman and M. Lautens, in *New Trends in Cross-Coupling: Theory and Applications*, ed. T. J. Colacot, The Royal Society of Chemistry, Cambridge, 2015, pp. 276–321; (e) D. A. Petrone, J. Ye and M. Lautens, *Chem. Rev.*, 2016, **116**, 8003–8104; (f) D. J. Jones, M. Lautens and G. P. McGlacken, *Nat. Catal.*, 2019, **2**, 843–851. See also recent reviews on catalytic carbohalogenation of carbon–carbon multiple bonds: (g) D. Bag, S. Mahajan and S. D. Sawant, *Adv. Synth. Catal.*, 2020, **362**, 3948–3970; (h) D. Bag, H. Kour and S. D. Sawant, *Org. Biomol. Chem.*, 2020, **18**, 8278–8293.
- R. F. Heck, *J. Am. Chem. Soc.*, 1968, **90**, 5538–5542.
- (a) Y. Tamaru, M. Hojo, H. Higashimura and Z.-I. Yoshida, *Angew. Chem., Int. Ed. Engl.*, 1986, **25**, 735–737; (b) Y. Tamaru, M. Hojo, S. Kawamura and Z.-I. Yoshida, *J. Org. Chem.*, 1986, **51**, 4089–4090. A related reaction was also reported, see: (c) J. P. Parrish, Y. C. Jung, S. I. Shin and K. W. Jung, *J. Org. Chem.*, 2002, **67**, 7127–7130.
- (a) D. Kalyani and M. S. Sanford, *J. Am. Chem. Soc.*, 2008, **130**, 2150–2151; (b) D. Kalyani, A. D. Satterfield and M. S. Sanford, *J. Am. Chem. Soc.*, 2010, **132**, 8419–8427.
- (a) Y. He, Z. Yang, R. T. Thornbury and F. D. Toste, *J. Am. Chem. Soc.*, 2015, **137**, 12207–12210; (b) J. Miró, C. del Pozo, F. D. Toste and S. Fustero, *Angew. Chem., Int. Ed.*, 2016, **55**, 9045–9049.
- (a) E. P. A. Talbot, T. A. Fernandes, J. M. McKenna and F. D. Toste, *J. Am. Chem. Soc.*, 2014, **136**, 4101–4104; Recently, Pd-catalyzed 1,2-arylfluorination of internal enamides was reported: (b) Y. Xi, C. Wang, Q. Zhang, J. Qu and Y. Chen, *Angew. Chem., Int. Ed.*, 2021, **60**, 2699–2703.
- For selected examples of Pd-catalyzed 1,2-addition of $C(sp^2)$ –I bonds to alkenes, see: (a) S. G. Newman and M. Lautens, *J. Am. Chem. Soc.*, 2011, **133**, 1778–1780; (b) H. Liu, C. Li, D. Qiu and X. Tong, *J. Am. Chem. Soc.*, 2011, **133**, 6187–6193; (c) S. G. Newman, J. K. Howell, N. Nicolaus and M. Lautens, *J. Am. Chem. Soc.*, 2011, **133**, 14916–14919; (d) X. Jia, D. A. Petrone and M. Lautens, *Angew. Chem., Int. Ed.*, 2012, **51**, 9870–9872; (e) D. A. Petrone, H. A. Malik, A. Clemenceau and M. Lautens, *Org. Lett.*, 2012, **14**, 4806–4809; (f) D. A. Petrone, M. Lischka and M. Lautens, *Angew. Chem., Int. Ed.*, 2013, **52**, 10635–10638; (g) D. A. Petrone, H. Yoon, H. Weinstabl and M. Lautens, *Angew. Chem., Int. Ed.*, 2014, **53**, 7908–7912; (h) Z.-M. Zhang, B. Xu, L. Wu, L. Zhou, D. Ji, Y. Liu, Z. Li and J. Zhang, *J. Am. Chem. Soc.*, 2019, **141**, 8110–8115; (i) X. Chen, J. Zhao, M. Dong, N. Yang, J. Wang, Y. Zhang, K. Liu and X. Tong, *J. Am. Chem. Soc.*, 2021, **143**, 1924–1931.
- For selected examples of Ni-catalyzed 1,2-addition of $C(sp^2)$ –I bonds to alkenes, see: (a) H. Yoon, A. D. Marchese and M. Lautens, *J. Am. Chem. Soc.*, 2018, **140**, 10950–10954; (b) A. D. Marchese, F. Lind, Á. E. Mahon, H. Yoon and M. Lautens, *Angew. Chem., Int. Ed.*, 2019, **58**, 5095–5099; (c) A. D. Marchese, L. Kersting and M. Lautens, *Org. Lett.*, 2019, **21**, 7163–7168; (d) A. D. Marchese, T. Adrianov, M. F. Köllen, B. Mirabi and M. Lautens, *ACS Catal.*, 2021, **11**, 925–931.
- H. Liu, C. Chen, L. Wang and X. Tong, *Org. Lett.*, 2011, **13**, 5072–5075.
- (a) C. M. Le, P. J. C. Menzies, D. A. Petrone and M. Lautens, *Angew. Chem., Int. Ed.*, 2015, **54**, 254–257; (b) Y. H. Lee and B. Morandi, *Angew. Chem., Int. Ed.*, 2019, **58**, 6444–6448.



14 (a) T. Takahashi, D. Kuroda, T. Kuwano, Y. Yoshida, T. Kurahashi and S. Matsubara, *Chem. Commun.*, 2018, **54**, 12750–12753; (b) T. Takahashi, T. Kurahashi and S. Matsubara, *ACS Catal.*, 2020, **10**, 3773–3777.

15 Pd-catalyzed 1,3-alkynylbromination of norbornene with alkynyl bromides, see: Y. Li, X. Liu, H. Jiang, B. Liu, Z. Chen and P. Zhou, *Angew. Chem., Int. Ed.*, 2011, **50**, 6341–6345.

16 Au-catalyzed 1,2-alkynylhalogenation of alkenes with alkynyl halides, see: (a) M. Kreuzahler and G. Haberhauer, *J. Org. Chem.*, 2019, **84**, 8210–8224; (b) M. E. de Orbe, M. Zanini, O. Quimonero and A. M. Echavarren, *ACS Catal.*, 2019, **9**, 7817–7822; (c) P. D. García-Fernández, C. Izquierdo, J. Iglesias-Sigüenza, E. Díez, R. Fernández and J. M. Lassaletta, *Chem.-Eur. J.*, 2020, **26**, 629–633.

17 The reaction of **1a** with $^3\text{BuMe}_2\text{Si}$ -protected alkynyl bromide gave the corresponding 1,1-alkynylbromination product in 51% NMR yield. The use of $^3\text{Pr}_3\text{Si}$ -protected alkynyl chloride instead of **2** were less effective for the reaction with **1a** (14% NMR yield). See also the ESI† for details.

18 J. Le Bras and J. Muzart, *Tetrahedron*, 2012, **68**, 10065–10113.

19 J. Tsuji, *Synthesis*, 1984, 369–384.

20 When the reaction of **1a** with **2** was performed, the formation of 2-acetylnaphthalene was observed by ^1H NMR analysis of the crude reaction mixture (2% NMR yield).

21 For a related discussion on the Pd-catalyzed 1,1-difunctionalization of terminal alkenes, see: (a) K. B. Urkalan and M. S. Sigman, *Angew. Chem., Int. Ed.*, 2009, **48**, 3146–3149; (b) V. Saini, L. Liao, Q. Wang, R. Jana and M. S. Sigman, *Org. Lett.*, 2013, **15**, 5008–5011; (c) M. Orlandi, M. J. Hilton, E. Yamamoto, F. D. Toste and M. S. Sigman, *J. Am. Chem. Soc.*, 2017, **139**, 12688–12695.

22 A. Tenaglia, K. Le Jeune, L. Giordano and G. Buono, *Org. Lett.*, 2011, **13**, 636–639.

23 R. F. Heck, *J. Am. Chem. Soc.*, 1969, **91**, 6707–6714.

24 This result was different from our expectation based on the reaction mechanism shown in Scheme 7. See Scheme S1 in the ESI† for the detailed discussion.

25 I. Kalvet, K. J. Bonney and F. Schoenebeck, *J. Org. Chem.*, 2014, **79**, 12041–12046.

26 DFT calculations indicated that the Pd catalyst bearing **2'** as a ligand provided an energetically favorable reaction pathway in comparison with that containing **1b** as a ligand. See the ESI† for details.

27 Despite many attempts, we have failed to find a TS for the reductive elimination with inversion of the configuration at the propargylic carbon atom at this stage.

28 (a) T. Nishida, S. Ogoshi, K. Tsutsumi, Y. Fukunishi and H. Kurosawa, *Organometallics*, 2000, **19**, 4488–4491. Stoichiometric study on the reactivity of π -allenyl Pd complex was also reported: (b) K. Tsutsumi, S. Ogoshi, S. Nishiguchi and H. Kurosawa, *J. Am. Chem. Soc.*, 1998, **120**, 1938–1939.

29 (a) E. D. Glendening, A. E. Reed, J. E. Carpenter, and F. Weinhold, *NBO Version 3.1*; (b) A. E. Reed, L. A. Curtiss and F. Weinhold, *Chem. Rev.*, 1988, **88**, 899–926.

